

# Optimization of Crush Initiators on Steel Front Rail of Vehicle

J. Marzbanrad<sup>\*1</sup>, M. Ebrahimi-F<sup>1</sup>, M. Khosravi<sup>2</sup>

1-School of Automotive Engineering, Iran University of Science and Technology, Tehran, Iran 2- Young Researchers and Elite Club, Borujerd Branch, Islamic Azad University, Borujerd, Iran

\* Corresponding Author

## Abstract

This paper focuses on the optimization of initiating dimensions of groove bearing in association with desired design of vehicle's front structure which is made up of low carbon steels in the case of frontal collision. Axial bearing analysis is done numerically using nonlinear finite element code LS-DYNA. In this analysis, changes of two main parameters including measure of energy absorption of structure and maximum force of structure collision are being considered. Square structure profile is being chosen and the grooves are placed on two opposite sides. Tests of collision simulation are performed for steel samples and then a mathematical equation is derived; next, the initiating dimensions are optimized using Genetic Algorithm. Desired case for design of this structure part is the one which provides maximum energy absorption measure and minimum collision force; in this paper, the most optimal case is an initiator with groove depth of 4.5 mm and radius of 10 mm.

**Keywords:** Bearing, Energy Absorber, Maximum Collision Force, Initiator of Groove Bearing, Vehicle Front Rail

## 1. Introduction

Transportation effect on human life, comfort and safety has become important with the increase of this industry in the world. Vehicles including ships, trains and planes have assigned a great part of transportation to themselves. A great number of people lose their lives due to transportation accidents annually; this makes designers to decrease injuries level by innovating modern methods [1]. 60% of accidents relate to vehicle frontal collision; this fact proves the necessity of effective components in this case. In frontal collision study, 40% of energy absorption is allocated to vehicle's front rail which turns this component to the most important one in frontal collisions safety [2]. Comprehensive experimental investigation on the response of composite sandwich panels to quasi-static compression has been carried out in pervious researches [3-5]. The crashworthiness parameters, namely the peak load, absorbed crash energy, specific absorbed energy, average crushing load, stroke efficiency, and crush force efficiency of

various types of composite sandwich panels were investigated in a series of edgewise compression tests. Also, the response of low-velocity impact has been determined based on mass ratio, which is defined as the ratio of the impact mass to effective mass of the structural component.

The front rail is the most important part of vehicle structure which can improve the parameters of collision force and energy absorption simultaneously. In the case that the front rail is high rigid, the passenger deceleration will be increased which may cause the passenger to be thrown and collided to the windshield. Unlike, if the structure is weak, it can be bended easily which decreases the energy absorption which can also hurt the passenger [6]. This article [7] describes an investigation into the material and structural requirements of an automotive frontal protection system (FPS). The operation of the FPS relies both on cantilever bending and local crush of the structure at the impact point to absorb the required energy.

Fig (1) shows a view of vehicle's front rail. In addition to structure roles in tolerating loads such as

engine and gearbox, and road loads as the support of suspension system, this component has the role of accident energy absorption as an absorber. This component begins from firewall and ends to the front bumper.

Since this component must be considered rigid as far as possible to bear bending and torsion loads, this problem is in opposition with increase of energy absorption characteristic. Moreover, in the case of component bending during collision in one point, the engine and its accessories will move towards the passenger which creates critical situation. If the vehicle structure is designed in such a way that can provide maximum energy absorption of collision, this problem can be solved to some extent [6, 9].

In general, axial crush response has been investigated with respect to types of response modes, geometry-material design criteria for components, crush characteristics to evaluate performance, methods to initiate or modify response and rate and temperature effects. Researchers have also investigated effects of material type, material alloying, and process parameters on the axial crush response of metallic alloy components [10-13]. An experimental investigation was performed to study the effects of ambient temperature on axial-crush response of steel, square box components by Dipaolo and Tom [13]. They show that depending on the material type, secondary folding-phase load and energy-absorption crush characteristics can be significantly influenced by ambient temperature. Also, in [14] a specific axial crush configuration

response of steel, square box components under quasi-static testing conditions has been studied. In [15, 16] the results from an experimental investigation into crushing characteristics of single, welded and plate divided mild steel tubes of varying lengths subjected to quasi-static and dynamic axial loading have been presented.

Song and et.al. [17] Introduced origami patterns to thin-walled structures and studied their axial crushing. Patterned tubes with square, hexagonal and octagonal sections are studied using FEA. Also in [18] Jandaghi and Marzbanrad studied the crush behavior of segmented circular tubes, made of aluminum alloy 6061 and subjected to quasi-static axial loading, analytically and experimentally. Crush behavior of Tailor-Made Tubes (TMTs) was modeled by integrating available analytical models and superposition principle. The effects of different TWB parameters, such as weld line locations and material combinations on crushing characteristics are studied in [19]. Such crushing characteristics as specific energy absorption, average crush force, peak force are also evaluated. The results exhibited the advantages of TWBs with a noticeable improvement in the peak force and energy absorption. Energy absorption and reaction force of S-rails that are made of transformation-induced plasticity (TRIP) or dual phase steel (DP) considering forming history has been studied in [20] and an optimum design for improving crash performance of the S-rail using trigger proposed.



**Fig1.**Front rail of Mazda [8]

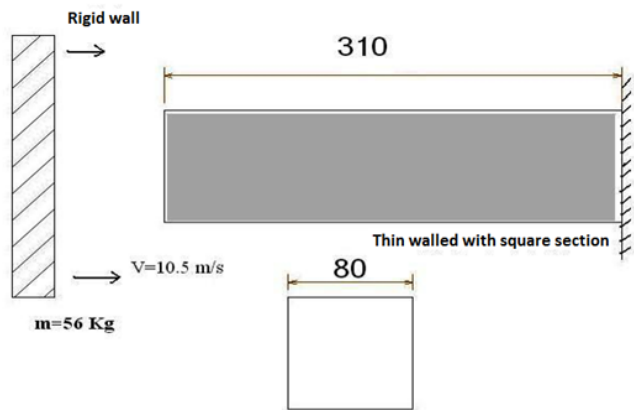


Fig2. A model of front rail collision to the rigid obstacle

Table 1. Specifications of material

| Material | Wall Thickness | Yield Stress | Tube Density | Increase Percent | Young Modulus |
|----------|----------------|--------------|--------------|------------------|---------------|
| St13     | 2              | 355          | 7840         | 18%              | 210           |



Fig3. Tensile and pressure test equipment and placement of sample under pressure

2. Test Conditions and Validation of Collision Finite Element Model

To analyze the energy absorption performance of vehicle’s front rail which acts as a thin-wall tube in collision study, dynamic model of collision is determined as demonstrated in Fig (2).

Dimensions and materials of all samples are the same. Square tube profile includes side of 80 mm, length of 310 mm and thickness of 2 mm. Specifications of used material are illustrated in Table (1).

As it is shown in Fig (2), the colliding body impacts the tube with velocity of  $v=15.5$  m/s and

Weight of 550 kg directly with zero angle. One side of profile is free and the other side is fixed in all orientations and degrees of freedom.

To validate the applied method in this paper, experimental methods have been used. Quasi static tests are done by the universal tensile and compression testing equipment (STM-150) with capacity of 150 KN and loading velocity of 5 mm/min. The samples are loaded axially between the equipment jaws and the load-displacement curve is derived.

Fig (3) shows quasi static test equipment and the way the sample is installed.

The actual stress-strain diagram of the applied material from tensile test is exhibited in Fig (4). This diagram is identified to the used software.

Width, thickness and length of tested square tubes are 25 mm, 1 mm and 200 mm, respectively. All the tubes are borne 145 mm with velocity of 5 mm/min. The first sample has no initiator, the second one has two initiators and third one has three initiators. Fig (5) shows the samples after bearing.

The comparison of experimental results and bearing simulation of samples 1, 2 and 3 are brought in Table (2).

The models are made in ANSYS software; boundary conditions and material specifications are allocated to them and then are solved in impact specialized software LS-DYNA. The element thin shell 163 is used for model meshing and the material is determined as nonlinear plastic. During bearing process, the contact friction coefficient of tube layers is considered 0.2.

Appropriate number of test samples is required for optimization. Since the optimization is performed on

dimensions of initiators, different measures are assigned to two main geometric parameters as independent variables to understand the effect of those measures change on output results which are dependent variables of the problem.

As it is seen in Fig (6), two independent variables are the measure of dent ( $y$ ) and curve radius ( $R$ ) of the initiator. The distance from initiators beginning to the beam front is constant for all samples and in equal to 60 mm.

Moreover, dependent variables include the measure of collision energy absorption and maximum collision force. To improve structure characteristics in accidents, the maximum collision force must be decreased while structure energy absorption must be increased as far as possible. In the case of not using initiator, the structure must be reinforced to increase energy absorption which leads to maximum force increase. Thus, correct and optimal use of initiators not only helps in energy absorption but also decreases the collision force significantly.

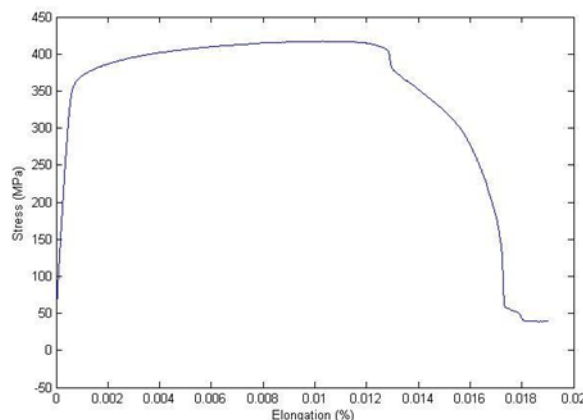


Fig4. Actual stress-strain diagram from tensile test

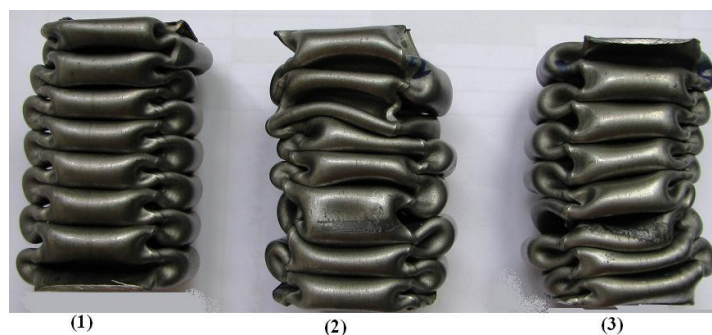
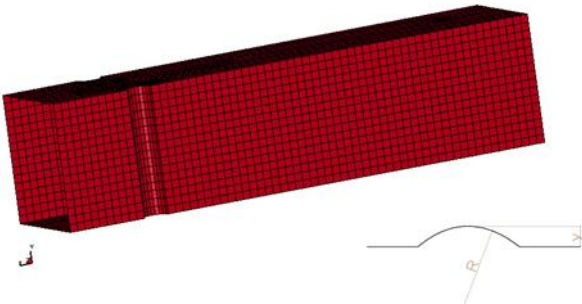


Fig5. Tested steel tubes after bearing

**Table 2.** Comparison of experimental and bearing simulation results of samples 1, 2 and 3

| Sample | Experimental Test Results |                | Simulation Results |               | Difference (Percent)  |                      |
|--------|---------------------------|----------------|--------------------|---------------|-----------------------|----------------------|
|        | $F_{mean}(KN)$            | $F_{max} (KN)$ | $F_{mean}(KN)$     | $F_{max} KN)$ | $\Delta F_{mean} (%)$ | $\Delta F_{max} (%)$ |
| 1      | 8.76                      | 25.04          | 10.45              | 23.69         | 19.1                  | 5.3                  |
| 2      | 9.53                      | 22.2           | 9.95               | 20.4          | 4.4                   | 8.1                  |
| 3      | 10.17                     | 23.5           | 11.21              | 20.86         | 10.2                  | 11.2                 |



**Fig6.** Schematic of the model and analyzed parameters

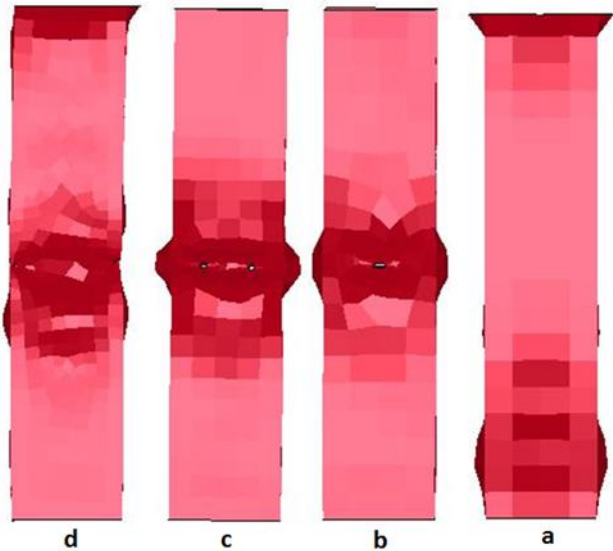


**Fig7.** Collision with zero angle a) without initiator, b) one hole, c) 2 hole, d) 4 hole

In order to investigate the initiator effects on collision results, four cases has been considered. Figure 7 depicts the zero angle collision results after 1.3ms for each case. In the first case (a), without initiator, bearing starts in both ends of rod, whenever by adding initiator in the middle of rod, failure occurs around initiators. In case b there is a long hole and cases c, d have two and four holes respectively.

In the next stage, to assess the collision angle, angle has been changed to 15 degree for each above mentioned cases. Results are compared in figure 8 after 3ms.

As shown in figure 8, unlike the zero angle collision, in this situation, bearing occurs in both ends of all cases. Also results indicate that with increasing the collision angle, getting started bearing is less dependent on location of initiators.



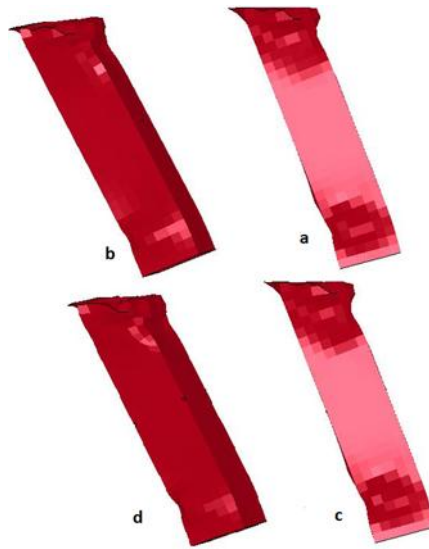


**Fig8.** Collision with 15o angle a) without initiator, b) one hole, c) 2 hole, d) 4 hole

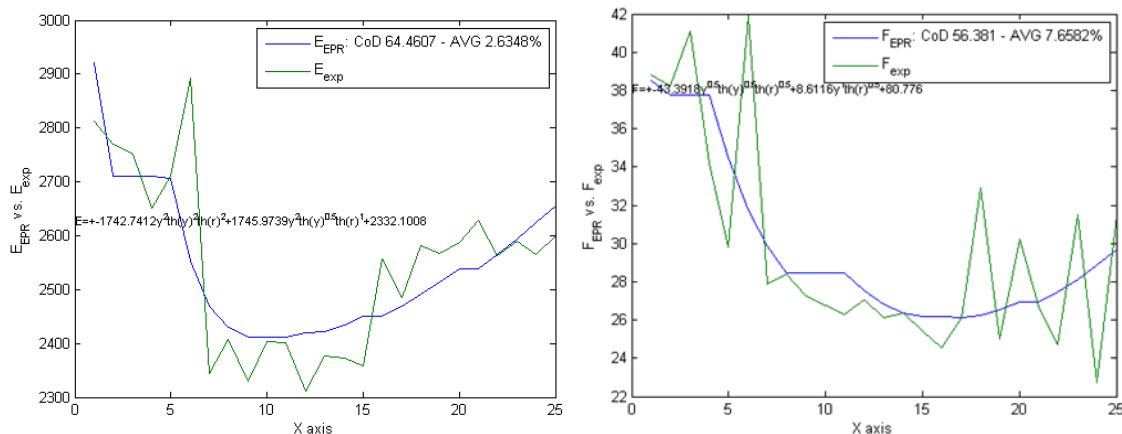


**Fig9.** Function and curve of energy absorption for actual and predicted measures of EPR (Left)

**Fig10.** Function and curve of maximum collision force for actual and predicted measures of EPR (Right)

### 3. Optimization and Discussion of Collision Tests Results

Initiators dimensions and simulations results for different samples have been presented in table (3). Using the code of EPR which is written in MATLAB software, the change of dependent variables versus independent variables is shown in Fig (9) and Fig (10). It should be noted that the desired curve is calculated and estimated by Genetic Algorithm.

As it can be seen from Table (3) results, the maximum measure of collision force and energy absorption of the structure decreases with the increase of y measure in most cases. This is also true for curve

radius with less intensity. It is also observed that the structure is more sensitive to y parameter than R parameter from output results of Genetic Algorithm for each level.

Both parameters y and R are analyzed simultaneously in optimization part by using multi objective optimization method. Optimization results demonstrate that the most optimal values for simultaneous optimization of energy absorption and maximum force of collision for y and R are 4.5 mm and 10 mm, respectively. Fig (11) illustrates comparison of force-displacement curve for simple and optimal initiators cases. Fig (12) shows the

sample with initiator before and after bearing. Considering this figure, two deformations are made in

the tubes and the third deformation is about to be made.

**Table 3.** Simulation results of samples collision

| Test Number | Y (mm) | R (mm) | Maximum Force (KN) | Absorbed Energy (J) |
|-------------|--------|--------|--------------------|---------------------|
| 1           | 2      | 2      | 161.57             | 17019               |
| 2           | 2      | 7.5    | 148.69             | 16741               |
| 3           | 2      | 10     | 141.69             | 16842               |
| 4           | 2      | 15     | 147.08             | 17010               |
| 5           | 2.5    | 2.5    | 148.96             | 17010               |
| 6           | 3      | 3      | 150.83             | 16759               |
| 7           | 3.5    | 3.5    | 145.87             | 16860               |
| 8           | 4      | 4      | 142.69             | 16867               |
| 9           | 4      | 6      | 160.81             | 17031               |
| 10          | 4      | 6      | 160.82             | 17148               |
| 11          | 4      | 11     | 144.36             | 17065               |
| 12          | 4.5    | 4.5    | 144.29             | 17056               |
| 13          | 5      | 5      | 154.1              | 17094               |
| 14          | 5.5    | 5.5    | 146.05             | 17047               |
| 15          | 6      | 6      | 146.02             | 16891               |
| 16          | 6      | 8      | 155.25             | 16971               |
| 17          | 6.5    | 6.5    | 144.13             | 16977               |
| 18          | 7      | 7      | 145.22             | 16972               |
| 19          | 7.5    | 7.5    | 144.62             | 16980               |
| 20          | 8      | 8      | 151.45             | 17004               |
| 21          | 8      | 10     | 146.02             | 17152               |
| 22          | 8.5    | 8.5    | 147.15             | 17152               |
| 23          | 9      | 9      | 152.7              | 17163               |
| 24          | 9.5    | 9.5    | 151.22             | 17172               |
| 25          | 10     | 10     | 152.03             | 17328               |

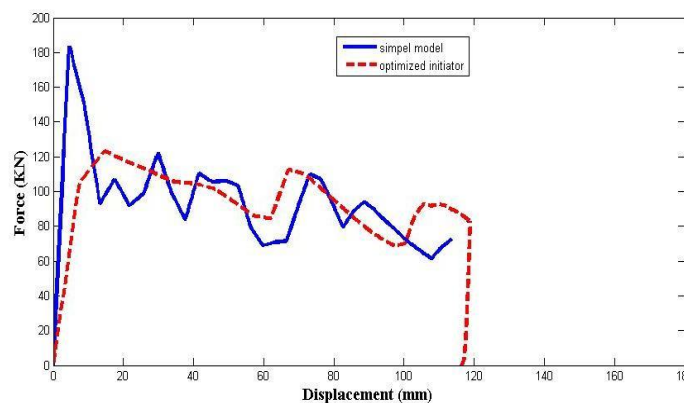


**Fig11.** Comparison of force-displacement curve for simple and optimal initiators samples

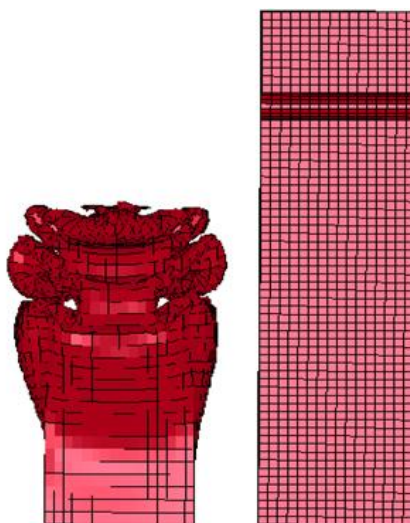


**Fig12.** Model with optimal initiator before and after deformation

### Conclusion

In this paper, grooved bearing initiators are used on the front steel rail of vehicle to improve effective parameters of passenger safety, and their geometric parameters are optimized multi objectively. To ensure the correctness of numerical analyses, quasi static experimental tests of some square tubes in the laboratory are used and the results are compared with numerical results and analyses. Of 25 simulation samples of collision, the geometric parameter of dent depth has the most effect on the output parameters. Generally, the more the parameters  $y$  and  $R$  are increased, the more the maximum collision force and the energy absorption of the structure are decreased. Therefore, considering the same value for both output parameters, optimal dimensions of 4.5 mm for dent depth and 10 mm for curve radius of bearing initiator are determined after the optimization.

### References

- [1]. Eren I., Gur Y. and Aksoy Z., "Finite element analysis of collapse of front side rails with new types of crush initiators", *International Journal of Automotive Technology*, vol. 10, issue 4, pp. 451-457, 2009.
- [2]. Zhang X.W., Tian Q.D. and Yu T.X., "Axial crushing of circular tubes with buckling initiators", *Thin-walled structures*, vol. 47, pp. 788-797, 2009.
- [3]. Tarlochan, F., Hamouda, A.M.S., Mahdi, E., Sahari, B.B., "Composite sandwich structures for crashworthiness applications", *Proceedings of the Institution of Mechanical Engineers, Part L: Journal of Materials: Design and Applications*, vol. 221, no. 2, pp. 121-130, 2007.
- [4]. Chai, G.B., Zhu, S., "A review of low-velocity impact on sandwich structures", *Proceedings of the Institution of Mechanical Engineers, Part L: Journal of Materials: Design and Applications*, vol. 225, no. 4, pp. 207-230, 2011.
- [5]. Okano, M., Sugimoto, K., Saito, H., Nakai, A., Hamada, H., "Effect of the braiding angle on the energy absorption properties of a hybrid braided FRP tube", *Proceedings of the Institution of Mechanical Engineers, Part L: Journal of Materials: Design and Applications*, vol. 219, no. 1, pp. 59-66, 2005.
- [6]. Gumruk R. and Karadeniz S., "A numerical study of the influence of bump type triggers on the axial crushing of top hat thin-walled



- section", *Thin-walled structures*, vol. 46, pp. 1094-1106, 2008.
- [7]. Brooks, R., "A Materials and Structure Perspective on the Feasibility of Automotive Frontal Protection Systems Meeting the Proposed Pedestrian Safety Test Criteria", *Proceedings of the Institution of Mechanical Engineers, Part L: Journal of Materials: Design and Applications*, vol. 220, no. 2, pp. 67-78, 2006.
- [8]. <http://www.carbodydesign.com/vehicles>
- [9]. Marzbanrad J., Mehdikhanlo M. and Saeedi Pour A., "An energy absorption comparison of square, circular, and elliptic steel and aluminum tubes under impact loading", *Turkish Journal of engineering and Environmental Science*, vol. 33, pp. 159-166, 2009.
- [10]. Kim H.S., "New extruded multi-cell aluminum profile for maximum crash energy absorption and weight efficiency", *Thin-walled Structures*, Vol. 40, pp. 311-327, 2002.
- [11]. Tarlochan, F., Samer, F., Hamouda, A.M.S. , Ramesh, S., Khalid K., "Design of thin wall structures for energy absorption applications: Enhancement of crashworthiness due to axial and oblique impact forces", *Thin-Walled Structures* Vol. 71, pp. 7-17, 2013.
- [12]. Seitzberger, M., Rammerstorfer, F.G., Gradinger, R., Degischer, H.P., Blaimschein, M., Walch, C., "Experimental studies on the quasi-static axial crushing of steel columns filled with aluminium foam", *International Journal of Solids and Structures*, vol. 37, pp. 4125-4147, 2000.
- [13]. DiPaolo, B.P. , Tom, J.G., "Effects of ambient temperature on a quasi-static axial-crush configuration response of thin-wall, steel box components", *Thin-Walled Structures* Vol. 47, Issues 8-9, , pp. 984-997, 2009.
- [14]. DiPaolo, B.P. , Tom, J.G., "A study on an axial crush configuration response of thin-wall, steel box components: The quasi-static experiments", *International Journal of Solids and Structures*, Vol. 43, Issues 25-26, , pp. 7752-7775, 2006.
- [15]. Ronchietto, F., Chung, S., Yuen, K., Nurick, G.N., "Response of axially stacked square tubes to axial impact loads", *Latin American Journal of Solids and Structures*, vol. 6, pp. 413 - 440, 2009.
- [16]. Velmurugan, R., Muralikannan, R., "Energy absorption characteristics of annealed steel tubes of various cross sections in static and dynamic loading", *Latin American Journal of Solids and Structures*, vol. 6, pp. 385 - 412, 2009.
- [17]. Song, J., Chen, Y., Lu, G., "Axial crushing of thin-walled structures with origami patterns", *Thin-Walled Structures*, Vol. 54, pp. 65-71, 2012.
- [18]. Jandaghishahi, V., Marzbanrad, J., "Analytical and experimental studies on quasi-static axial crush behavior of thin-walled tailor-made aluminum tubes", *Thin-Walled Structures* Vol. 60, pp. 24-37, 2012.
- [19]. Xu, F., Sun, G., Li, G., Li, Q., "Experimental study on crashworthiness of tailor-welded blank (TWB) thin-walled high-strength steel (HSS) tubular structures", *Thin-Walled Structures* Vol. 74, pp. 12-27, 2014.
- [20]. Hosseini-Tehrani, P., Asadi, E., "Effects of new materials on the crashworthiness of S-rails", *Proceedings of the Institution of Mechanical Engineers, Part L: Journal of Materials: Design and Applications*, vol. 222, no. 1, pp. 37-44, 2008.